X-Ray Study of the Correlations in the Thermal Fluctuations of Free-Standing Smectic-*A* Films

J. D. Shindler E. A. L. Mol, A. Shalaginov, and W. H. de Jeu

Stichting voor Fundamenteel Onderzoek der Materie, Institute for Atomic and Molecular Physics, Kruislaan 407, 1098 SJ Amsterdam, The Netherlands

(Received 29 August 1994)

The first quantitative experimental study is reported of the displacement-displacement correlations in the thermal fluctuations of freely suspended smectic-*A* films, performed by combining specular and diffuse x-ray scattering. For the first time we are able to separate the long wavelength thermal fluctuations from the local smectic disorder, and obtain a direct measure of the smectic bend and compression elastic constants as well as the surface tension. The local contribution to the total fluctuation profile is found to be considerable. The results are well described by the theory of Holyst [Phys. Rev. A **44**, 3692 (1991)].

PACS numbers: 61.30.–v, 61.10.Lx, 68.15.+e

A smectic liquid crystal may be described as a system which, apart from the long-range orientational order of the elongated molecules, exhibits one-dimensional translational ordering. Such a system is at its lower marginal dimensionality, so that the translational order is not truly long range but decays algebraically with position as $\mathbf{r}^{-\eta}$. If $u(\mathbf{r})$ is the layer displacement from its equilibrium position, $\langle u^2(\mathbf{r})\rangle$ is found to diverge logarithmically with sample size (Landau-Peierls instability) [1]. Freely suspended smectic films are unique model systems because they combine these properties with a controlled size and a high uniformity. In practice the film thickness can vary from two to a very large number of layers. Thin films of these phases allow the investigation of the effects of reduced dimensionality and free surfaces on the film structure.

Recently, theoretical models of free-standing smectic films have been developed [2,3] that extend the smectic bulk free energy (which depends on B and K, the elastic constants for compression and bending of the smectic layers, respectively) to include the effect of the surface tension γ at the boundaries. Taking $\mathbf{r} = (\mathbf{R}, z)$ with z along the film normal, these surface terms occur for $z = 0$ and $z = Nd \equiv L$, where N is the number of smectic layers with spacing d, and L is the total film thickness. Central to the theory is the calculation of the layer displacement fluctuations $\sigma^2(0, z) = \langle u^2(0, z)\rangle$ and of the displacement-displacement correlation function $C(\mathbf{R}, z, z') = \langle u(\mathbf{R}, z')u(0, z)\rangle$. The fluctuation profile depends on the ratio $\nu = \gamma/\sqrt{BK}$; for $\nu > 1$ surface damping of the layer fluctuations is expected.

Freely suspended smectic films can be made large and flat enough for x-ray reflectivity measurements [4–6], which, however, only probe the laterally averaged density profile through the film. This Letter combines diffuse as well as specular x-ray reflectivity measurements of thin smectic-*A* films of various thicknesses. Measurements of the diffuse scattering have already been used to determine the height-height correlation function of liquid [7,8] and solid [9,10] surfaces, while recently a liquid crystal polymer film on a substrate has been studied [11]. In the latter case the layer fluctuations were dominated by the static undulations of the underlying substrate. In the case of freely suspended smectic films the nonspecular diffuse scattering probes the in-plane wave vector dependence of the fluctuations. This allows a direct determination of the displacement-displacement correlation function and thus of γ, B, and K. Once this is known we can obtain from the specular x-ray reflectivity the local (uncorrelated) contribution of the smectic disorder to the total fluctuation profile. We find it to be non-negligible compared to the long length scale thermal fluctuations.

The compound investigated, 5-heptyl-2-[4-(3, 3, 4, 4, 5, 5, 6, 6, 7, 7, 8, 8, 8-tridecafluorooctyl)-phenyl]-pyrimidine (FPP), is pictured in Fig. 1(a) and was obtained from

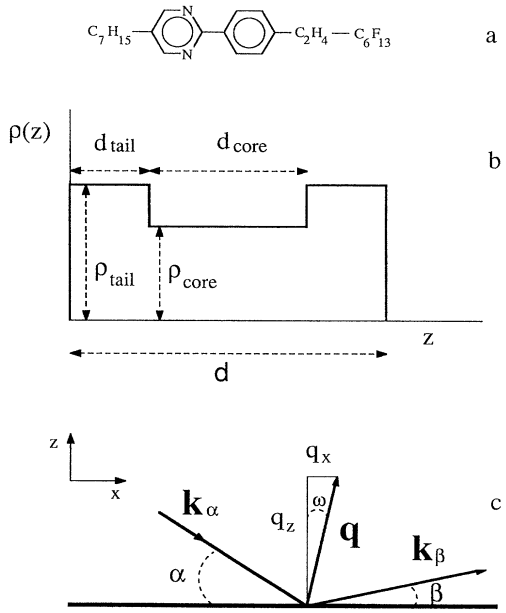

FIG. 1. (a) Chemical structure of FPP. (b) Model electron density profile for a single smectic layer. (c) Scattering geometry; the reciprocal space scattering vector is defined as $\mathbf{q} = \mathbf{k}_\beta - \mathbf{k}_\alpha$.

 0031-9007/95/74(5)/722(4)$06.00

Merck (Darmstadt, Germany). Its phase sequence is K 72 S_C 80 S_A 124 I (°C). Here K, S_C, S_A, and I denote the crystalline, smectic-C, smectic-A, and isotropic phase, respectively. Films were prepared between four razor blades on a 25 × 10 mm^2 rectangular holder at 120–124 °C. The sample was mounted in a two-stage oven, which was evacuated and sealed. Details of the ovens and film holders are described elsewhere [5]. During the experiment, the film was kept well into the smectic-A phase at 88.0 ± 0.1 °C.

Cu K_α x rays were obtained from a Rigaku RU-300H generator operated at 18 kW, hence wave number $|\mathbf{k}| = 4.07$ Å^{-1}. In the configuration used we obtain an incident beam intensity of 8×10^7 photons/s. Background scattering was in general less than 0.1 count/s. A schematic of the scattering geometry is shown in Fig. 1(c); details of the scattering configuration are described in [12]. It employs a bent graphite monochromator which focuses the beam in the out-of-plane direction onto the sample, giving a beam size of approximately 0.1 × 3 mm^2. The incident in-plane beam divergence $\Delta\alpha$ and the in-plane detector acceptance $\Delta\beta$ are defined by slits, chosen such that $\Delta\alpha = \Delta\beta$. Approximating these profiles by Gaussians, we can write the in-plane resolution function $R(\Delta\alpha, \Delta\beta) = R(\Delta q_\parallel)R(\Delta q_\perp)$. For $\Delta\beta = \Delta\alpha$ and small angles, the resolution width along the direction of $\mathbf{q}$ is given by $\Delta q_\parallel = \sqrt{2}\,k\Delta\alpha$, and the resolution width transverse to $\mathbf{q}$ by $\Delta q_\perp = (q_z/2k)\Delta q_\parallel$. For this work, $\Delta q_\parallel = 1.9 \times 10^{-3}$ Å^{-1}, and $\Delta q_\perp = 2.3 \times 10^{-4} q_z$. The sample mosaic is found to introduce a negligible broadening of the specular line width $\Delta q_\perp$. Out of the scattering plane [(z, x) plane] the resolution is poor due to the focusing of the monochromator and the widely set detector slits, $\Delta q_y \simeq 0.1$ Å^{-1}. Thus the intensity is effectively integrated over in this direction.

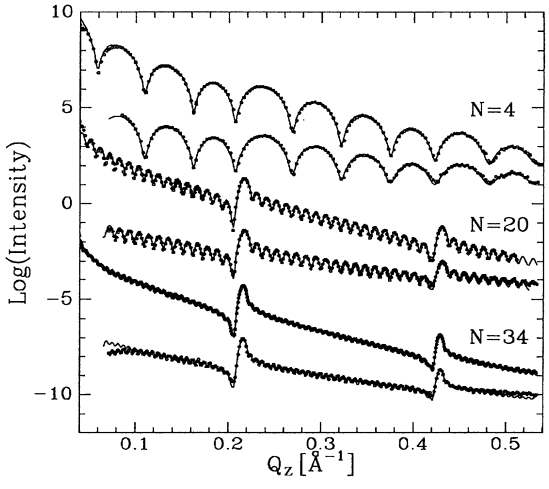

FIG. 2. Specular ($\omega = 0$, upper curves) and off-specular ($\omega = 0.15°$, lower curves) radial scans, with solid line fits as described in the text. Curves have been shifted for clarity.

Data paths were taken in both the radial and transverse directions. Radial scans correspond to setting the offset angle $\omega = (\beta - \alpha)/2$ fixed, and varying the total scattering angle $\alpha + \beta$. Specular ($\omega = 0$) and off-specular ($\omega = 0.15°$) radial scans for films of 4, 20, and 34 layers are shown in Fig. 2. Note the similarity of both types of scan indicating conformality between the two interfaces. Transverse rocking scans vary ω, keeping the total scattering angle $\alpha + \beta$ fixed. Figure 3 shows transverse scans for films of 4 and 34 layers, across the first and second Bragg peaks and at two intermediate q_z positions. When $\alpha \neq \beta$ radial and transverse scans are corrected for the changing footprint of the beam on the sample by multiplication by the factor $(2k/q_z)\sin\alpha$. All data have been scaled to the main beam intensity. Geometrical effects due to the size of the beam footprint in relation to the sample size and the sample area visible by the detector have been corrected for in the data. Background was calculated both from scans with no film present and from data for which $\alpha \leq 0$ or $\beta \leq 0$. In practice, transverse scans are background subtracted while the radial scans have a constant background added to the model.

Following Refs. [2(b),13], consistent with the first Born approximation but including refraction, the intensity can be written in the form

$$\frac{I(\mathbf{q})}{I_0} = \left\{ |R_F|^2 \exp(-q_z'^2\sigma_{\mathrm{loc}}^2)\,\frac{\Delta q_\perp}{\sqrt{2\pi}} \int_{-\infty}^{\infty} dx \times \exp(iq_x x)\exp\left[-\tfrac{1}{2}x^2(\Delta q_\perp)^2\right] G(x, q_z') \right\} \otimes \exp\left[-\tfrac{1}{2}q_\parallel^2/(\Delta q_\parallel)^2\right], \quad (1)$$

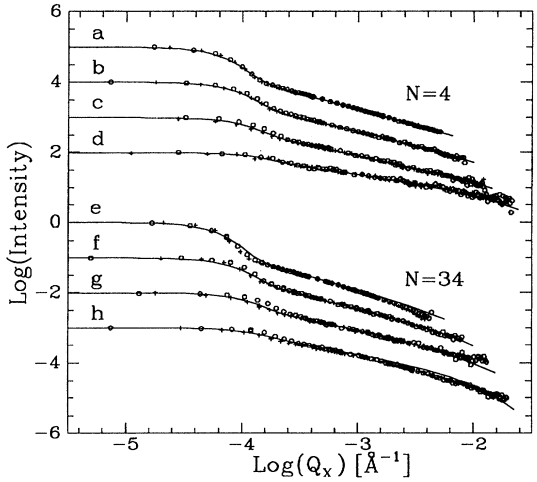

FIG. 3. Transverse scans at fixed q_z, with solid line fits as discussed in the text; circles and crosses indicate positive and negative q_x, respectively. (a)–(d) q_z values of 0.235, 0.292, 0.348, and 0.448 Å^{-1}, respectively; (e)–(h) q_z values of 0.216, 0.287, 0.355, and 0.429 Å^{-1}, respectively. Curves have been shifted for clarity.

where

$$G(x, q_z') = \sum_{m,n}^{N} \exp[iq_z'(m-n)d] \exp[-q_z'^2 g_{mn}(x)/2]. \quad (2)$$

The average z component of the wave vector transfer in the film is $q_z' = (q_z^2 - q_c^2)^{1/2}$, with q_c defined as the critical wave vector transfer for total reflection. The $|R_F|^2$ term is an exact calculation of the Fresnel reflectivity of a single layer using the slab model of Fig. 1(b). It is smeared with a Gaussian of width $\sigma_{\rm loc}$, which approximates the local (short wavelength) contribution to the total fluctuations. Note that the two-dimensional resolution convolution over $(\Delta q_\parallel, \Delta q_\perp)$ is performed as a one-dimensional convolution (denoted as $\otimes$) along $q_\parallel$ with width $\Delta q_\parallel$, and a real space cutoff of $1/\Delta q_\perp$ to the structure factor integration along x (taken here as an approximation to $\perp$). Finally, $g_{mn}(x) = g(x, z_m, z_n)$, with $z_j = [j - \frac{1}{2}(N+1)]d$, is the full correlation function which is calculated directly instead of $C(x, z, z')$. It is given by $g(x, z, z') = \langle [u(x, z') - u(0, z)]^2 \rangle = \sigma^2(x, z') + \sigma^2(0, z) - 2C(x, z, z')$. While each of the right hand terms diverge with increasing films size and hence require an additional cutoff, this is not the case for $g(x, z, z')$. We find the analytical form of Ref. [3(b)] most computationally efficient. It can be written as

$$g(x, z, z') = \frac{k_B T}{8\pi\sqrt{KB}} \int_0^{\xi_0} d\xi \, \frac{1}{\xi[(1+\nu)^2 - (1-\nu)^2 \exp(-2\xi)]} \times \left[f(\xi, 2z, z_0) + f(\xi, 2z', z_0) - 2J_0\left(\sqrt{\xi}\,\frac{x}{\sqrt{\lambda L}}\right) f(\xi, z_+, z_-) \right], \quad (3)$$

where $\xi_0 = L\lambda(2\pi/a_0)^2$, $\lambda = \sqrt{K/B}$, a_0 is a lateral intermolecular distance, $z_+ = z + z'$, and $z_- = |z - z'|$ (with minimum value z_0). J_0 is the Bessel function of order zero, while the function f is given as

$$f(\xi, z_+, z_-) = 2(1-\nu^2)\exp(-\xi)\cosh(\xi z_+/L) + (1+\nu)^2 \exp(-\xi z_-/L) + (1-\nu)^2 \times \exp[-\xi(2 - z_-/L)].$$

Choosing the cutoff $z_0 \simeq d/4$ gives essentially the same results as in Ref. [2]. Also, for this choice of $z_0 \geq a_0$, the correlation function is not sensitive to the value of a_0. The specular component is the result of finite resolution, since the sample size is much larger than the coherence length of the x rays projected on the sample surface. This cutoff to the integral in terms of the effective coherence length allows a calculation of $g_{mn}(x)$ without use of a resolution determining cutoff [14,7].

In the fitting procedure we have three groups of significant model parameters: $(N, d), (\gamma, K, B)$, and $(\sigma_{\rm loc}, d_{\rm tail}, \rho_{\rm tail}/\rho_{\rm core})$. All but N are given a single value for modeling the data at all film thicknesses. The second group is related to the hydrodynamic fluctuations and the third group [see Fig. 1(b)] to the local smectic (dis)order. N and d can be extracted directly from the specular reflectivity curve positions of the Bragg peaks and the Kiessig fringes, respectively. We find $d = 29.40 \pm 0.04$ Å, independent of layer position and film thickness, which is about equal to the length of a fully stretched molecule. After fixing N and d, we have fit the transverse line shapes at fixed q_z varying only γ, K, and B. Best fits for all films occur for values of $\gamma = (13.0 \pm 0.5) \times 10^{-3}$ N/m, $K = (1.0 \pm 0.5) \times 10^{-11}$ N, and $B = (1.0 \pm 0.5) \times 10^9$ N/m^2. Fits using these values are given as the solid lines in Fig. 3. Fits to the specular and off-specular radial scans (Fig. 2) were then performed with only the third group $(\sigma_{\rm loc}, d_{\rm tail}, \rho_{\rm tail}/\rho_{\rm core})$ as adjustable parameters. We find $\sigma_{\rm loc} = 2.6$ Å, $d_{\rm tail} = 0.19d$, and $\rho_{\rm tail}/\rho_{\rm core} = 1.14$. These values are essentially independent of both layer number and film thickness.

In this system, there is remarkable agreement between the model and the data, using the same parameters for every thickness film. This even applies to the thinnest films where the continuum model is assumed less valid. However, careful scrunity of the data shows somewhat unexpectedly deviations from the model for thicker films at higher q values. This is clearest in the transverse line shapes at the Bragg positions in q_z [Figs. 3(e) and 3(h)], which cannot be fit by only varying B and K. Off Bragg peak transverse scans of the same film [Figs. 3(f) and 3(g)] are fit better by the model. The Bragg positions are characterized by constructive interference of the summand in Eq. (2) with $m \neq n$. Hence these deviations could indicate that the mechanism of coupled fluctuations across smectic layers is more complicated than the model.

The value of 13×10^{-3} N/m obtained for the surface tension is considerably smaller than anticipated, as all data reported so far lie in the range $(20-26) \times 10^{-3}$ N/m [15(a)]. This could be related to the specific properties of the fluorinated chain, which is bulkier and stiffer than a hydrogenated chain. This idea is substantiated by recent measurements on compounds with fluorinated chains similar to FPP where values of the order of 14×10^{-3} N/m have been found [15(b)]. The value for K is quite normal compared to other systems [1]. On the other hand, the lower limit we can set for B is about 2 orders of magnitude above values reported for other smectic-A systems [16]. However, most of these published data are for systems that have a smectic-A to nematic

phase transition. Clearly our FPP system is nearly incompressible, with layers fluctuating in unison down to very short in-plane modes. As a result $\nu \ll 1$, and the profile of the hydrodynamic (collective) fluctuations along z is very flat.

The value of $\sigma_{\mathrm{loc}} = 2.6$ Å for the local fluctuations is to be compared with $\sigma_{\mathrm{tot}} = 4.6$ Å as obtained from a standard slab model to fit the specular reflectivity. Both σ_{loc} and σ_{tot} are independent of N. Using $\sigma_{\mathrm{tot}}^2 = \sigma^2 + \sigma_{\mathrm{loc}}^2$, this gives $\sigma = \sigma(0, z) = 3.8$ Å for the hydrodynamic part of the fluctuations. It is clear that the local fluctuations add a non-negligible contribution to the total fluctuation profile, and that the approximation that these can be neglected [2,6] is not generally valid. The fitted value of $\rho_{\mathrm{tail}}/\rho_{\mathrm{core}}$ is 1.14, while from simple molecular modeling a difference between ρ_{tail} and ρ_{core} of the order of 50% would be expected. In addition, d_{tail} is also smaller than anticipated. Connecting the model to a more detailed picture of the molecular conformations will be the subject of a future paper.

In conclusion, we have quantitatively determined for the first time the correlations in the thermal fluctuations of thin smectic-A films. This is accomplished by measuring via the off-specular x-ray scattering the in-plane wave vector dependence of the hydrodynamic (collective) fluctuations which is governed by the elastic parameters. This is to be contrasted with results reported so far for the specular scattering only, which depends only weakly on the fluctuations. All data (specular, off-specular, and transverse scans) can be fitted by a single set of parameters. In addition, we have separated the magnitude of the collective thermal fluctuations from the extent of local smectic disorder. Unlike common belief we found the latter to add a non-negligible contribution.

This work is part of the research program of the Stichting voor Fundamenteel Onderzoek der Materie [Foundation for Fundamental research on Matter (FOM)] and was made possible by financial support from the Nederlandse Organisatie voor Wetenschappelijk Onderzoek [Netherlands Organization for the Advancement of Research (NWO)].

[1] See, for example, G. Vertogen and W. H. de Jeu, *Thermotropic Liquid Crystals, Fundamentals* (Springer, Berlin, 1988).
[2] (a) R. Holyst, D. J. Tweet, and L. B. Sorensen, Phys. Rev. Lett. **65**, 2153 (1990); (b) R. Holyst, Phys. Rev. A **44**, 3692 (1991); (c) A. Poniewierski and R. Holyst, Phys. Rev. B **47**, 9840 (1993).
[3] (a) V. P. Romanov and A. N. Shalaginov, Sov. Phys. JETP **75**, 483 (1992); (b) A. N. Shalaginov and V. P. Romanov, Phys. Rev. E **48**, 1073 (1993).
[4] G. S. Smith, C. R. Safinya, D. Roux, and N. A. Clark, Mol. Cryst. Liq. Cryst. **144**, 235 (1987).
[5] (a) S. Gierlotka, P. Lambooy, and W. H. de Jeu, Europhys. Lett. **12**, 341 (1990); (b) P. Lambooy, S. Gierlotka, I. W. Hamley, and W. H. de Jeu, in *Phase Transitions in Liquid Crystals*, edited by S. Martellucci and A. N. Chester (Plenum, New York, 1992), Chap. 17.
[6] D. J. Tweet, R. Holyst, B. D. Swanson, H. Stragier, and L. B. Sorensen, Phys. Rev. Lett. **65**, 2157 (1990).
[7] M. K. Sanyal, S. K. Sinha, K. G. Huang, and B. M. Ocko, Phys. Rev. Lett. **66**, 628 (1991).
[8] I. M. Tidswell, T. A. Rabedeau, P. S. Pershan, and S. D. Kosowsky, Phys. Rev. Lett. **66**, 2108 (1991).
[9] D. E. Savage, J. Kleiner, N. Schimke, Y. H. Phang, T. Janowski, J. Jacobs, R. Kariotis, and M. G. Lagally, J. Appl. Phys. **69**, 1 (1991).
[10] R. Schlatmann, J. D. Shindler, and J. Verhoeven (to be published).
[11] R. E. Greer, R. Shashidhar, A. F. Thibodeaux, and R. S. Duran, Phys. Rev. Lett. **71**, 1391 (1993).
[12] J. D. Shindler, and R. M. Suter, Rev. Sci. Instrum. **63**, 5343 (1992).
[13] S. K. Sinha, E. B. Sirota, S. Garoff, and H. B. Stanley, Phys. Rev. B **38**, 2297 (1988).
[14] P. Dutta, and S. K. Sinha, Phys. Rev. Lett. **47**, 50 (1981).
[15] (a) T. Stoebe, P. Mach, and C. C. Huang, Phys. Rev. E **49**, R3587 (1994); (b) C. C. Huang, (private communication).
[16] M. Benzekri, J. P. Marcerou, H. T. Nguyen, and J. C. Rouillon, Phys. Rev. B **41**, 9032 (1990).